MAGNETIC RESONANCE IN CHEMISTRY, VOL. 31, 632–638 (1993)

Substituent Effects on ESR Parameters of α-Phenyl-*N*-*tert*-butylnitrone Spin Adducts. Resolution Enhancement and Mass Spectrometry

Kai Pan, Chiou-Rong Lin and Tong-Ing Ho*
Department of Chemistry, National Taiwan University, Roosevelt Road, Section 4, Taipei, Taiwan

The combination of high-performance liquid chromatography (HPLC) and ESR spectrometry was used to isolate the free radicals produced by the reaction of a Grignard reagent with 15 substituted α-phenyl-*N*-*tert*-butylnitrones. Long-range hyperfine splitting constants (hfsc) were obtained by the resolution enhancement method. Linear correlation studies between hfsc and Hammett σ_p constants are reported. Dual-parameter correlations using σ_R and σ_I were also studied. The mass spectra for the HPLC-isolated spin adducts and their fragmentation patterns are reported.

KEY WORDS ESR Spin adducts Spin trapping Mass spectrometry α-Phenyl-*N*-*tert*-butylnitrones

INTRODUCTION

Spin trapping has been shown[1–3] to be an important technique in many fields of chemistry.[4–9] The advantage of this technique is to convert unstable or short-lived free radicals into more stable aminoxyl radicals for which ESR spectra can be easily recorded. In cases when several trapped free radicals are in the reaction mixture, the free radical chromatographic method[10–15] allows the separation of the mixture and the ability to study each trapped radical unambiguously. Recent studies on improving the structure determination of spin-trapped radicals include gas chromatography–mass spectrometry (GC–MS),[11] trimethylsilylated spin adduct GC–MS,[16] double spin adduct liquid chromatography (LC)–MS,[10] MS,[17–20] resolution enhancement[21–23] and the application of new type of spin traps.[3]

We have reported on the trapping of 1,2-diphenylethyl radicals by 2-methyl-2-nitrosopropane (MNP) in the photochemical reaction of substituted *trans*-stilbene and amines[24] and have observed linear Hammett correlations for the nitrogen and proton hyperfine splitting constants (hfsc). These aminoxyl radicals can also be prepared by adding benzylmagnesium halide to α-phenyl-*N*-*tert*-butylnitrones (PBNs).[25] The substituted PBNs shown were prepared and reacted with various Grignard reagents to generate the corresponding aminoxyl radicals, which were examined by high-performance liquid chromatographic (HPLC)–ESR–MS and resolution enhancement techniques. We report Hammett-type correlations between hfsc and substituent constants and the mass fragmentation pattern for the HPLC-isolated spin adducts.

* Author to whom correspondence should be addressed.

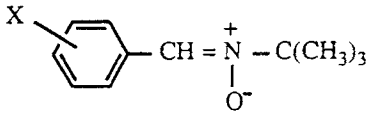

1–15

X = *p*-OMe (**1**), *p*-Me (**2**), *p*-Pr^i (**3**), *m*-Me (**4**), H (**5**), *m*-OMe (**6**), *p*-Cl (**7**), *p*-Br (**8**), *m*-Cl (**9**), *m*-Br (**10**), *p*-CF_3 (**11**), *m*-CN (**12**), *m*-NO_2 (**13**), *p*-CN (**14**), *p*-NO_2 (**15**)

EXPERIMENTAL

The substituted PBNs were prepared according to the known procedure.[26,27] The melting points were as follows: **1**, 95–97; **2**, 69–71; **3**, 101–103; **4**, 69–70; **5**, 71–72; **6**, 90–91; **7**, 71–72; **8**, 60–62; **9**, 76–77; **10**, 78–79; **11**, 81–83; **12**, 92–93; **13**, 108–110; **14**, 161–162; **15**, 147–149 °C.

The Grignard reagents were of commercial grade (Aldrich). Ethyl acetate and hexane used for HPLC–ESR were of spectroscopic grade (Merck). The ESR spectrometer (Bruker ESR 300 X-band) was equipped with an ER 035M NMR gaussmeter and the *g* value was measured with DPPH ($g = 2.003\,63$) as internal standard and using a dual-cavity probe. The ESR spectrometer was operated at 100 kHz modulation frequency and 9.76 GHz microwave and was connected to a Perkin–Elmer JPLC system with a silica gel column. A quartz flow cell of *ca.* 0.5 mm i.d. and 3 cm long was set in the EPR sample cavity and was connected to the exit of the column with *ca.* 0.3 mm i.d. Teflon tubing. A 1 : 5 mixture of ethyl acetate and hexane was used as the eluent. The chromatographic conditions were pressure *ca.* 100 kg cm^{-2}, flow-rate 1.0 ml min^{-1} and temperature *ca.* 25 °C. The microwave power was 12 dB (6.3 mW).

0749–1581/93/070632–07 $08.50

Received 6 November 1992
Accepted (revised) 24 February 1993

For HPLC–ESR, the magnetic field was fixed at the centre peak maxima and the magnetic field modulation was applied at an amplitude of 7 G to cover a wide range during the separation of radicals. By using a resolution enhancement technique with Fourier transform deconvolution,[21–23] which can be calculated on the Bruker 300 computer, the resolution-enhanced ESR spectra of HPLC-isolated spin adducts (e.g. benzyl adducts **17e**) are obtainable (see Fig. 2). The computer-simulated spectra are in good agreement with the observed spectra. Several long-range hfsc including γ-H and *o*-H for the phenyl ring were obtained for the first time for a series of benzyl spin adducts **16e–30e** (see Table 6). The coupling constants of the *o*- and γ-protons were determined as follows: for *m*-CH_3, *m*-OCH_3, *m*-Cl, *m*-Br, *m*-CN and *m*-NO_2 compounds, there are two *ortho*-proton couplings, which have similar values. For example, for the *m*-CH_3 compound, the two *ortho*-proton couplings are 0.802 and 0.795 G then the γ-proton (2H) can be assigned as the smaller value of 0.787 G. For all the *meta*-substituted compounds the γ-protons (2H) are all assigned as the smaller values. For the *para*-substituted compounds, there are two identical *ortho*-protons and γ-protons. In order to be consistent with the *meta*-substituted data, our assignment is that the smaller values are for the γ-proton. The supporting evidence for the assignment is seen from the linear correlation of the *ortho*-protons with σ_p [$r = 0.980$, Eqn (6)], and the correlation of the γ-proton with all σ values ($r = 0.947$).

The mass spectrometer (Finnigan) was operated at 70 or 20 eV ionization potential. Infrared spectra were recorded with a Perkin–Elmer Model 7000 spectrometer.

RESULTS

The results of all the experiments are given in Figs. 1–3 and Tables 1–6.

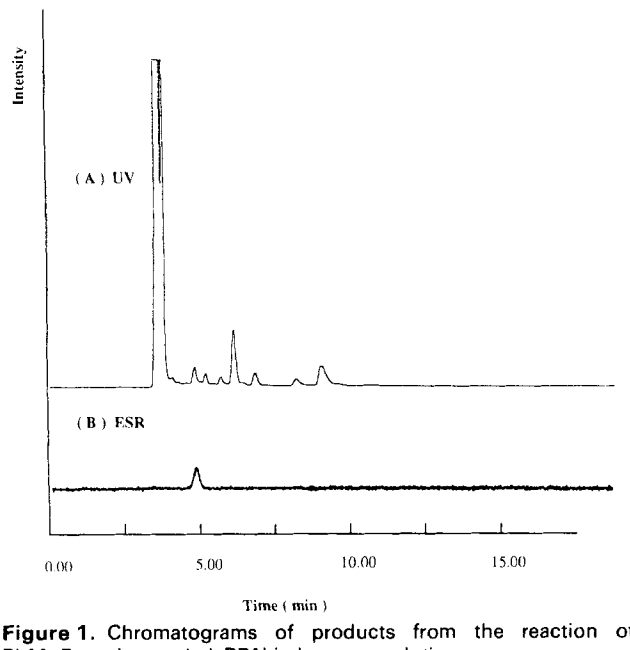

Figure 1. Chromatograms of products from the reaction of PhMgBr and *p*-methyl-PBN in benzene solution.

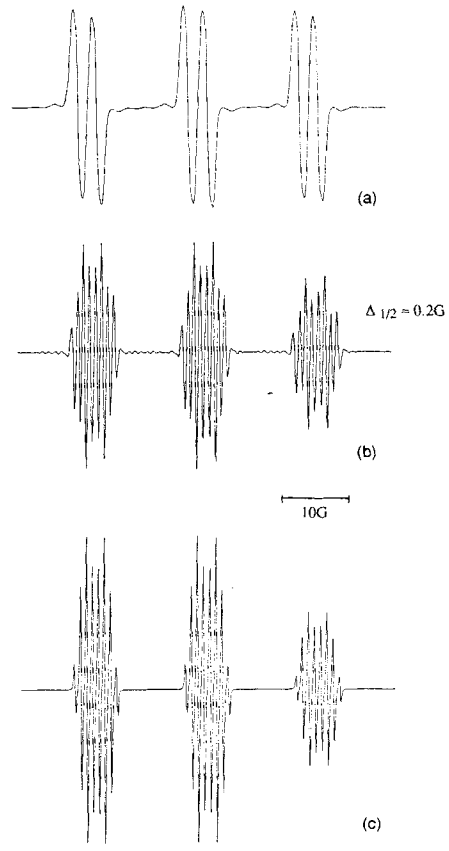

Figure 2. (a) EPR spectrum of product **17e**; (b) resolution-enhanced spectrum from (a); (c) simulated spectrum of (b).

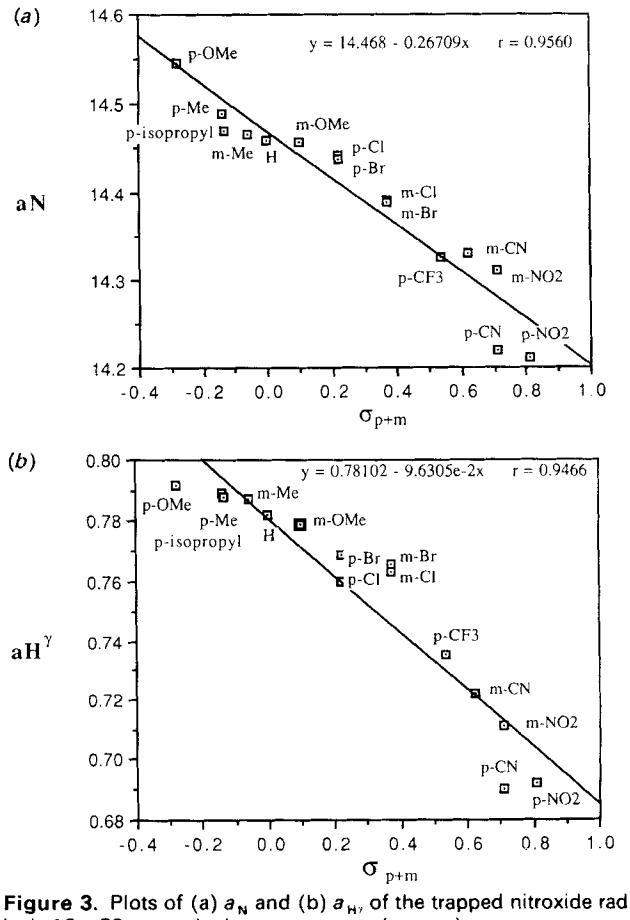

Figure 3. Plots of (a) a_N and (b) $a_{H\gamma}$ of the trapped nitroxide radicals **16e–30e** *vs.* substitutent constant (σ_p, σ_m).

Table 1. Hyperfine splitting constants a_N (in gauss ± 0.05 G) of adducts of substituted α-phenyl-*N*-*tert*-butylnitrones (X-PBNs) with various radicals in benzene

X in X-PBN	R in RMgBr C_6H_5	n-C_4H_9	C_2H_5	CH_3	$C_6H_5CH_2$	$CH_2{=}CHCH_2$
p-OMe	14.48	14.73	14.75	14.96	14.62	14.70
p-Me	14.45	14.66	14.60	14.92	14.60	14.64
p-Pr^i	14.46	14.67	14.62	14.93	14.58	14.61
m-Me	14.46	14.63	14.63	14.83	14.46	14.63
H	14.43	14.63	14.58	14.85	14.58	14.62
m-OMe	14.43	14.63	14.63	14.81	14.46	14.62
p-Cl	14.42	14.62	14.58	14.83	14.55	14.56
p-Br	14.42	14.62	14.58	14.79	14.56	14.58
m-Cl	14.33	14.61	14.58	14.76	14.45	14.52
m-Br	14.34	14.60	14.57	14.78	14.44	14.50
m-CN	14.40	14.58	14.46	14.74	14.46	14.50
m-NO_2	14.43	14.48	14.50	14.73	14.46	14.53
p-CN	14.38	14.55	14.49	14.88	14.43	14.58
p-NO_2	14.38	14.50	14.48	14.63	14.43	14.63

Table 2. Hyperfine β-H splitting constants a_H (in gauss ± 0.05 G) of adducts of substituted α-phenyl-*N*-*tert*-butylnitrones (X-PBNs) with various radicals in benzene

X in X-PBN	R in RMgBr C_6H_5	n-C_4H_9	C_2H_5	CH_3	$C_6H_5CH_2$	$CH_2{=}CHCH_2$
p-OMe	2.25	3.16	3.25	3.48	2.58	3.13
p-Me	2.28	3.19	3.40	3.51	2.45	3.12
p-Pr^i	2.15	3.19	3.25	3.49	2.55	3.17
m-Me	2.23	3.47	3.39	3.67	2.46	3.31
H	2.24	3.15	3.30	3.61	2.59	3.17
m-OMe	2.23	3.31	3.41	3.73	2.48	3.25
p-Cl	2.13	3.02	3.10	3.29	2.49	2.86
p-Br	2.22	2.98	3.07	3.20	2.39	3.00
m-Cl	2.14	2.97	3.04	3.13	2.31	2.90
m-Br	2.13	2.98	3.05	3.12	2.30	2.90
m-CN	2.11	2.97	3.06	3.25	2.26	2.93
m-NO_2	2.13	2.65	2.80	2.97	2.46	3.13
p-CN	2.20	3.31	3.85	3.85	2.73	3.41
p-NO_2	2.13	2.84	2.95	3.05	2.45	3.08

Table 3. *g* Values (±0.0001) of adducts of substituted α-phenyl-*N*-*tert*-butylnitrones (X-PBNs) with various radicals in benzene

X in X-PBN	R in RMgBr C_6H_5	n-C_4H_9	C_2H_5	CH_3	$C_6H_5CH_2$	$CH_2{=}CHCH_2$
p-OMe	2.0066	2.0061	2.0065	2.0060	2.0066	2.0064
p-Me	2.0068	2.0066	2.0059	2.0064	2.0066	2.0059
p-Pr^i	2.0067	2.0060	2.0061	2.0058	2.0068	2.0067
m-Me	2.0066	2.0058	2.0056	2.0067	2.0067	2.0066
H	2.0061	2.0064	2.0065	2.0067	2.0060	2.0056
m-OMe	2.0066	2.0064	2.0059	2.0060	2.0063	2.0067
p-Cl	2.0066	2.0064	2.0063	2.0061	2.0058	2.0065
p-Br	2.0059	2.0066	2.0062	2.0059	2.0062	2.0062
m-Cl	2.0066	2.0064	2.0058	2.0063	2.0065	2.0062
m-Br	2.0064	2.0063	2.0057	2.0065	2.0066	2.0065
m-CN	2.0063	2.0068	2.0062	2.0067	2.0063	2.0066
m-NO_2	2.0062	2.0065	2.0057	2.0061	2.0066	2.0061
p-CN	2.0065	2.0060	2.0059	2.0061	2.0066	2.0061
p-NO_2	2.0061	2.0069	2.0060	2.0060	2.0062	2.0062

Table 4. Mass fragments (*m/z*; relative intensity, %) of phenyl radical adduct system

Product	Fragment					
	M^+	$[M-1]^{+\cdot}$	$[M-Bu^t]^+$	$[M-Bu^t-O-H]^+$	$[M-Bu^t-NO]^+$	$(CH_3)_3C^+$
p-OMe	284	283	227	210	197	57
	(0.90)	(2.60)	(9.31)	(5.33)	(100)	(4.66)
p-Me	268	267	211	194	181	57
	(2.10)	(8.10)	(36.66)	(33.23)	(100)	(17.68)
p-Pr^i	296	295	239	222	209	57
	(3.70)	(12.96)	(6.79)	(3.71)	(100)	(43.56)
H	254	253	197	180	167	57
	(0.91)	(1.30)	(33.11)	(31.09)	(100)	(9.01)
p-Cl	288	287	231	214	201	57
	(2.61)	(7.30)	(60.01)	(4.04)	(100)	(16.01)
p-Br	—	333, 331	277, 275	260, 258	247, 245	57
		(6.69)	(69.00)	(35.99)	(100)	(84.75)
p-CF_3	322	321	265	248	235	57
	(3.20)	(5.10)	(48.11)	(2.33)	(100)	(34.22)
p-CN	279	278	222	205	192	57
	(12.16)	(13.30)	(10.00)	(9.40)	(100)	(41.01)
p-Pr^i	234	233	177	162	147	57
(Methyl radical)	(1.70)	(13.26)	(60.23)	(18.71)	(100)	(78.11)

Table 5. Mass fragments (*m/z*; relative intensity, %) of benzyl radical adduct system

Product	Fragment			
	M^+	$[M-Bu^t+H]^+$	$[M-Bu^t-NO]^+$	$(CH_3)_3C^+$
p-OMe	298	242	211	57
	(1.98)	(23.04)	(100)	(17.57)
p-Me	282	226	195	57
	(29.98)	(4.04)	(100)	(12.57)
p-Pr^i	310	254	223	57
	(24.67)	(3.04)	(100)	(24.57)
H	238	212	181	57
	(1.22)	(2.04)	(100)	(34.57)
p-Cl	302	246	211	57
	(26.98)	(8.04)	(100)	(67.57)
p-Br	348, 346	292, 290	261, 259	57
	(34.62)	(12.90)	(100)	(43.33)
p-CF_3	336	280	249	57
	(4.98)	(10.04)	(49.87)	(100)
p-CN	293	237	206	57
	(4.45)	(11.04)	(70.87)	(100)

Table 6. Nitrogen, β-H and long-range hfscs of benzyl spin adducts 16e–30e obtained by resolution enhancement and simulation[a]

	a_N	β	γ	*o*-	*o*-	*p*-	σ_m, σ_p
p-OMe	14.546	2.496	0.792	0.801	—	—	−0.28
p-Me	14.489	2.403	0.789	0.798	—	—	−0.14
p-Pr^i	14.471	2.408	0.788	0.797	—	—	−0.13
m-Me	14.465	2.395	0.787	0.795	0.802	0.975	−0.06
H	14.459	2.394	0.782	0.794	—	0.722	0
m-OMe	14.458	2.381	0.779	0.788	0.792	0.973	0.10
p-Cl	14.442	2.346	0.760	0.789	—	—	0.22
p-Br	14.438	2.344	0.769	0.788	—	—	0.22
m-Cl	14.391	2.266	0.763	0.784	0.783	0.961	0.37
m-Br	14.388	2.263	0.766	0.786	0.785	0.963	0.37
p-CF_3	14.326	2.297	0.735	0.785	—	—	0.53
m-CN	14.330	2.199	0.722	0.780	0.774	0.960	0.62
m-NO_2	14.310	2.451	0.711	0.774	0.775	0.958	0.71
p-CN	14.220	2.256	0.690	0.783	—	—	0.71
p-NO_2	14.210	2.251	0.692	0.781	—	—	0.81

[a] Hyperfine splitting constants (hfscs) are in gauss ± 0.005 G, the deviation range from several experiments.

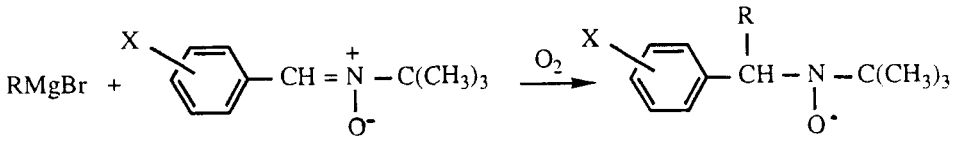

(1)

1–15 **16–30 (a–f)**

R = C_6H_5 (**a**), n-C_4H_9 (**b**), C_2H_5 (**c**)
CH_3 (**d**), $C_6H_5CH_2$ (**e**), $CH_2{=}CHCH_2$ (**f**)

The phenyl (**a**), n-butyl (**b**), ethyl (**c**), methyl (**d**), benzyl (**e**) and allyl (**f**) spin adducts were prepared by adding the corresponding Grignard reagents to the substituted PBNs (**1–15**) in benzene solution, followed by air oxidation [Eqn (1)]. All of the spin adducts show the same type of ESR spectra, namely triplets of doublets.

The reaction mixtures were subjected to HPLC separation with both UV and ESR detection, with ethyl acetate–hexane (1 : 5) as eluent. The chromatogram for a typical reaction system is shown in Figure 1. (R = C_6H_5, X = p-Me). The peak which gave rise to the ESR signal was separated and the EPR spectra were recorded in benzene solution. The hyperfine splitting constants for nitrogen (Table 1) and the β-proton (Table 2) were recorded. The g value of the spin adducts were determined by comparison with a small solid sample of 1,1-diphenyl-2-picryhydrazyl (DPPH) (g = 2.00363), the value are between 2.0068 to 2.0057 and summerized in Table 3.

Table 4 summarizes the major mass fragmentations for the phenyl spin adducts. Fragmentation patterns for other spin adducts were similar. For example, the methyl radical adduct (R = CH_3, X = p-$(CH_3)_2CH$) was shown to have the major fragmentations of $[M - t\text{-BuNO}]^+$ (100%), $[(CH_3)_3C]^+$ (78.11%), $[M - t\text{-Bu}]^+$ (60.23%), $[M - t\text{-BuOH}]^+$ (18.71%), $[M - 1]^+$ (13.26%) and $[M]^+$ (1.70%). The fragmentation pattern for the benzyl spin adducts (Table 5) is slightly different with the appearance of $[M - t\text{-Bu} + H]^+$. The presence of $[M - t\text{-Bu}]^+$, $[M - t\text{-BuNO}]^+$ (100%) and $[(CH_3)_3C]^+$ peaks is similar to the other spin adducts.

Using the resolution enhancement technique more hfscs in the ESR spectrum were obtained [Fig. 2(b)]; the measured hfscs were in good agreement with the computer-simulated spectra. All the nitrogen β-H and long-range hfscs of benzyl spin adducts **16e–30e** are summarized in Table 6. For the *meta* substituents, there are two different hfscs for the o-H. For the *para* substituents there is only one hfsc for o-H and the value is similar to that of the *meta* substituents. The γ-H hfscs have smaller values than the o-H hfscs. All of the hfsc values (β-H, γ-H and o-H of the phenyl group) decrease with increasing electron-withdrawing substituents. It is also found that both nitrogen and β-H hfscs are different from the previously obtained values without resolution enhancement.

The infrared spectra for the spin adducts indicate N–O• stretching at *ca.* 1000–1300 cm^{-1} and N–O• bending at 800 cm^{-1}. The N–O• stretch is of lower energy than the original PBN N–O stretching (1140–1180 cm^{-1}), which is indicative of the greater single bond character for the aminoxyl radical N—O• bond.

DISCUSSION

The obtained nitrogen and β-H hfscs are all consistent with the literature values for methyl,[3] n-butyl,[28] ethyl,[29] phenyl,[30] benzyl[3] and allyl[31] spin adducts with PBNs. The methyl, n-butyl and ethyl spin adducts showed large nitrogen and β-H hfsc. For all the spin adducts studied, the value of the nitrogen hfsc decreases with increasing electron-withdrawing capability of the *para* substituents of the phenyl group (Table 1). This trend is similar to the previous observation for similar aminoxyl radicals.[28,32–35] In contrast to the nitrogen hfsc, the β-H hfscs for all the systems studied do not have Hammett correlations with σ_p or σ_m constants. This non-linearity has been attributed to a through-space dipole–dipole interaction between the substituents and the benzylic C—H bond that alters the spin density at the hydrogen which affects the coupling between hydrogen and the radical.[32] The β-H hfscs are relatively small. The methine proton hfsc value is 1–5 Gauss.[34] The β-H hfscs can be used to calculate the dihedral angle between the nitrogen π-orbital and the N—C—H plane by using the Heller–McConnell equation:[36]

$$AH^{\beta} = B_1 + B_2 \cos^2 \theta \qquad (2)$$

where B_1 and B_2 are constants ($B_1 \approx 0$ and $B_2 \approx 26$ G for aminoxyl radicals). Thus smaller β-H hfsc correspond to larger θ value. The benzyl spin adducts with β-H hfscs of 2.30–2.59 G correspond to a time-average θ of 70°. The phenyl spin adducts possess smaller β-H hfscs hence θ is large, whereas, the alkyl spin adducts possess larger β-H hfscs, which correspond to smaller θ. In general, the electron-withdrawing substituents make the β-H hfsc smaller. Janzen *et al.*[37] reported that the phenyl ring tends to align with the nitroxyl p–π orbital. Our results are in agreement with their observations and indicate that electron-withdrawing groups may enhance the nitroxyl p–π and phenyl π orbital interaction.

The a_N, $a_{H\gamma}$ values which were obtained by the resolution enhancement technique are linearly correlated with Hammett σ_p and σ_m values (Fig. 3) with the following equations:

$$a_N = 14.468 - 0.267\sigma \qquad (r = 0.956) \qquad (3)$$

$$a_{H\gamma} = 0.781 - 9.630\sigma \qquad (r = 0.947) \qquad (4)$$

For the $a_{H\beta}$, a fair linear relationship is obtained without the m-NO_2:

$$a_{H\beta} = 2.389 - 0.223\sigma \qquad (r = 0.930) \qquad (5)$$

Even the *o*-H for the phenyl ring show some correlation with the σ_p value:

$$a_{H^o} = 0.794 - 0.018\sigma_p \qquad (r = 0.980) \qquad (6)$$

The slope of the Hammett plot for the nitrogen and β-H are similar but the slope for γ-H is more sensitive to the perturbation caused by the substituents [Eqn (4) with a slope of 9.63]. This may be due to the alternating polarization effect for the dominant resonance structure with positive charge at the nitrogen atom. The dual substituent parameter (DSP)[38] method provides important additional information not obtainable from a single-parameter treatment, viz. the relative magnitudes of the σ_I and σ_R, which allows one to determine differential changes in polar (σ_I) and resonance (σ_R) effects. DSP analysis on the γ-H hfsc indicated that the resonance and inductive effects are of equal importance:

$$a_{H\gamma} = 0.778 - 0.092\sigma_I - 0.083\sigma_R \qquad (r = 0.989) \quad (7)$$

$$a_{H\gamma} = 0.777 - 0.099\sigma_I - 0.120\sigma_{R^o}(\text{Taft}) \quad (r = 0.975) \quad (8)$$

The mass spectrometric data for the molecular and fragment ions provide the most useful information for the identification of these relatively stable aminoxyl radicals isolated by HPLC. For the phenyl spin adducts **16a–30a**, the fragmentation patterns (Table 4) can be systematically analysed owing to their regularity. The spin adducts gave relatively weak, albeit observable, molecular ions (M^+). The presence of stronger $[M - H]^{+\cdot}$ odd-electron ions may be due to the easy loss of the β-H atom. For all of the substituted spin adducts, the common base peak of $[M - t\text{-BuNO}]^+$ indicates the easy loss of the neutral *t*-BuNO from the molecular ion. The M − 57 peaks, corresponding to the loss of a *tert*-butyl radical, is the next most abundant fragmentation. Abe *et al.*[16] also observed the $[M - 57]^+$ ion peaks from the mass spectrum of bistrimethylsilylated hydroxyl spin adduct of PBN isolated by GC–MS. The $[M - t\text{-BuOH}]^+$ ion fragment originates from the loss of a *tert*-butyl alcohol and results in the formation of the $(XC_6H_4)(C_6H_5)CH{=}N^+$ fragment. This structure has also been observed by Abe *et al.*[16] For the mass spectra of alkyl spin adducts **16d–30d**, the fragmentation patterns are similar to those of the phenyl spin adduct (Table 4).

The mass spectra for the benzyl spin adducts **16e–30e** are different to those of the phenyl or alkyl spin adducts mentioned above. The presence of a stronger parent ion and $[M - t\text{-Bu} + H]^+$ fragments are unique. The presence of the base peak of $[M - t\text{-BuNO}]^+$ and the *tert*-butyl cation peak is similar to the previously discussed cases. This pattern is applicable to all the substituted spin adducts examined.

CONCLUSION

The HPLC–ESR technique can provide pure aminoxyl spin adducts for detailed scrutinization including resolution enhancement studies and mass spectral documentation. Long-range hfsc including γ-H and phenyl proton hfscs are obtained. Hammett correlations were obtained for a_N, $a_{H\beta}$ and $a_{H\gamma}$. The $a_{H\gamma}$ are more sensitive to the perturbations caused by the substituents. For the β-H hfsc, the more electron-withdrawing the substitutent, the larger is the dihedral angle θ. HPLC–ESR–MS provides useful structural information on the aminoxyl spin adducts obtained. The mass spectral analysis indicates that the $[M - t\text{-BuNO}]^+$ base peak is present for all the radicals studied. The mass spectral data provided unambiguous structural information for the aminoxyl radical trapped by PBN. The IR spectra for the aminoxyl radicals were also obtained and indicated that the N–O· stretching at around 1000–1300 cm^{-1}.

Acknowledgement

Financial support (NSC82-0208-M002-018) from the National Science Council of the ROC (Taiwan) is grateful acknowledged.

REFERENCES

1. E. G. Janzen, *Acc. Chem. Res.* **4**, 31 (1971).
2. M. J. Perkins, *Adv. Phys. Org. Chem.* **17**, 1 (1980).
3. D. L. Haire, U. M. Oehler, P. H. Krygsman and E. G. Janzen, *J. Org. Chem.* **53**, 4535 (1988).
4. K. Stolze, D. R. Duling and R. P. Mason, *J. Chem. Soc., Chem. Commun.* 268 (1988).
5. H. Kaur, K. H. W. Leung and M. J. Perins, *J. Chem. Soc., Chem. Commun.* 142 (1981).
6. A. Rockenbauer, M. Gyor and F. Tudos, *Tetrahedron Lett.* **27**, 3425 (1986).
7. N. Ohto, E. Niki and Y. Kamiya, *J. Chem. Soc., Perkin Trans. 2* 1770 (1977).
8. H. Chandra, I. M. T. Davidson and M. C. R. Symons, *J. Chem. Soc., Faraday Trans. 1* **79**, 2705 (1983).
9. A. Mackor, A. J. Wajer and Th. J. De Boer, *Tetrahedron* **24**, 1623 (1968).
10. E. G. Janzen, P. H. Krygsman, D. A. Lindsay and D. L. Haire, *J. Am. Chem. Soc.* **112**, 8279 (1990).
11. E. G. Janzen, P. H. Krygsman and D. L. Haire, *Biomed. Environ. Mass Spectrom.* **15**, 111 (1988).
12. E. G. Janzen, J. K. Weber, D. L. Haire and D. M. Fung, *Anal. Lett.* **18**(A14), 1749 (1985).
13. H. J. Stronks, E. G. Janzen and J. R. Weber, *Anal. Lett.* **17**(A4), 321 (1984).
14. K. Makino, F. Moryia and H. Hatano, *J. Chromatogr.* **332**, 71 (1985).
15. H. Iwahashi, Y. Negoro and A. K. R. Ikeda, *J. Chromatogr.* **391**, 119 (1987).
16. K. Abe, H. Suezawa and M. Hirota, *J. Chem. Soc., Perkin Trans. 2* 29 (1984).
17. A. Kazuhisa, S. Hironori, H. Minour and I. Tetsuo, *J. Chem. Soc., Perkin Trans. 2* 29 (1984).
18. A. Morrison and A. P. Davies, *Org. Mass. Spectrom.* **3**, 353 (1970).
19. A. Morrison, M. D. Barraty and A. P. Daies, *Org. Mass Spectrom.* **8**, 43 (1978).
20. J. F. W. Keana, *Chem. Rev.* **78**, 39 (1978).
21. A. Hedberg and A. Ehrenberg, *J. Chem. Phys.* **48**, 4822 (1968).
22. K. Shimokoshi and R. N. Jones, *J. Appl. Spectrosc.* **31**, 67 (1983).
23. T. I. Ho, K. Nozaki, A. Naito, S. Okazaki and H. Hatano, *J. Chem. Soc., Chem. Commun.* 206 (1989).

24. C. R. Lin, C. N. Wang and T. I. Ho, *J. Org. Chem.* **56**, 5025 (1991).
25. E. G. Janzen and B. J. Blackburn, *J. Am. Chem. Soc.* **90**, 5909 (1968).
26. W. D. Emmons and A. S. Pagano, *Org. Synth. Coll.* **5**, 191 (1973).
27. W. D. Emmons, *J. Am. Chem. Soc.* **79**, 5739 (1957).
28. D. Rehorek, W. Winkler, R. Wagener and H. Hennig, *Inorg. Chim. Acta* **64**, L7 (1982).
29. H. Ji and G. Xu, *Huaxue Tongbao*, **1**, 32 (1986).
30. E. G. Janzen and C. A. Evans, *J. Am. Chem. Soc.* **97**, 205 (1975).
31. T. Matsuzaki, T. Uda, A. Kazusaka, G. W. Keulks and R. F. Howe, *J. Am. Chem. Soc.* **102**, 7511 (1980).
32. D. F. Church, *J. Org. Chem.* **51**, 1138 (1986).
33. D. Clarke, B. C. Gilbert and P. Hanson, *J. Chem. Soc., Perkin Trans. 2* 517 (1977).
34. K. Makino, *J. Phys. Chem.* **83**, 2520 (1979).
35. E. G. Janzen, *Acc. Chem. Res.* **2**, 279 (1969).
36. C. Heller and H. M. McConnell, *J. Chem. Phys.* **32**, 1535 (1960).
37. E. G. Janzen, U. M. Oehler, D. L. Haire and Y. Kotake, *J. Am. Chem. Soc.* **108**, 6858 (1986).
38. D. J. Craik, R. T. Brownlee and M. Sadek, *J. Org. Chem.* **47**, 657 (1982).